

GSA Data Repository 2019048

1. Coastal geomorphology and vertical deformation

The arrows on Figure 1B, representing the onshore location where Quaternary vertical deformation has been quantified are listed in table DR1. Measured rates location are not homogeneous and mostly localized on uplifting coastal areas, but deformation in Wallacea also include subsidence of the eastern Banda volcanic arc (Sandiford, 2008), uplift of much of the outer (non-volcanic) Banda arc (e.g., Harris et al., 2009; Roosmawati and Harris, 2009; Nguyen et al. 2013) and local uplift of the volcanic arc above possible slab tears and subduction reversal (Sandiford, 2008; Ely and Sandiford, 2010) as well as opening and subsidence of deep basins (e.g., Pholbud et al. 2012).

Vertical deformation in overall Sundaland is not homogeneous. Our study focused on the central Sunda shelf, where almost no tectonic deformation is recorded. However, vertical deformation has been recorded in the numerous sedimentary basins that surround the shelf (Pubellier and Morley, 2014, Mansor et al. 2014). Vertical deformation history in those basins last for the Eocene and present-day subsidence is associated with sedimentary loading and thermal activity (e.g., Pubellier and Morley, 2014 and reference therein). Uplift also occurred at the boundaries of Sundaland and is responsible for mountain belts that grow since the Miocene (e.g., Barisan mountains, Barber et al., 2005; Meratus mountains, Malay Peninsula). All along the fore-arc of the Sunda-Banda arc, tectonic activity records the interaction of the subducting and overriding plate, as shown for instance in Sumba (Fleury et al., 2009). Initial phases of uplift record the collision of Timor during Late Miocene (e.g., Spencer et al., 2016; Nguyen et al., 2013; Duffy et al., 2017), followed by the subduction of the Scott plateau less than 5 My ago, which ultimately determined the fate of the subducting Indo-Australian plate.

Mangroves are derived from the Giri et al., 2011 database. Uplifted sequences of Quaternary coral reefs have been extracted from geological maps (1:250 000) of the Indonesian Geological Survey. Modern coral reefs are derived from the Global Coral Reef Monitoring Network (GCRMN, 2011). Alluvial plains are defined by areas whose elevations is below 30m asl.

2. Coral reef numerical modeling

2.1 Modeling sequences of coral reefs

We designed a 2-D numerical code that simulates the formation of sequences of stacked coral reefs through time. The entire modelling protocol is described in details in Husson et al., (2018) to which the reader is referred to Eustatic sea-level oscillations during the last 430 ka (Walbroeck et al., 2002) set the maximum duration of the simulations. The initial morphology is defined by a uniform slope α that we vary between 0.2% and 2.5%. The model uses empirical laws for reef growth G , erosion E and clastic sedimentation S in a series of modules. They are variably excited, depending on relative sea level as dictated by the joint effects of sea level oscillations and vertical land motion, as well as the morphology of the foundation.

The reef growth module (G) computes a growth rate, which is defined by a fraction of the potential reef growth rate G^* (i.e. the maximum admissible value - the rate at which the reef would grow under optimal conditions). At any location along the 2D profile, reef growth is defined as a slope normal vector. The local growth rates is defined by the growth potential rate G^* to which two penalties apply, such that:

$$G = \gamma \times \zeta \times G^*, \quad (1)$$

where γ and ζ are respectively the vertical and horizontal penalty factors. The vertical penalty factor γ accounts for the depth dependence of reef growth, which declines down to a depth z_{max} , such that:

$$\gamma = \frac{1}{2} \left[1 + \cos \left(\frac{\pi h(s)}{z_{max}} \right) \right], \quad (2)$$

where $h(s)$ is the local depth along the profile. In addition, at depths shallower than z_{min} , the penalty coefficient linearly decreases upwards to 0 at the surface. The horizontal penalty factor ζ is computed in order to account for increasing turbidity and decreasing wave oxygenation shoreward, as both hamper reef growth. ζ ensures that the production is focussed at the reef crest. The horizontal distance to the open water ($x_{o\omega} - x$) (where $x_{o\omega}$ is defined by a minimal water depth $z_{o\omega}$), which is inserted into the penalty factor, such that:

$$\zeta = \frac{1}{2} \left[1 + \tan \left(\frac{x_{o\omega} - x}{\delta} \right) \right], \quad (3)$$

where δ sets the horizontal tension.

The erosion module (E) is based on an erosional potential E^* , expressed as an effective volume per unit time (and per unit length of coast, for the model is 2D). The erosional potential is dissipated from the open ocean towards the shore, and so the erosional residual power E_r gradually decrease shorewards. At each location along the profile, a fraction of E_r erodes the foundation. That fraction is defined as a function of true local depth $h(s)$ along the curvilinear profile s and a coefficient of bedrock erodibility K , such that:

$$\frac{\partial E_r}{\partial s} = K \times E_r \times \exp \left(-\frac{h(s)}{z_0} \right), \quad (4)$$

where z_0 is the typical depth of wave action. The remainder is computed at each step along the profile and resets E_r until the shore is reached, where the residual power $E^* - \int_s \frac{\partial E_r}{\partial s} ds$ serves to carve a 1 m high notch. All the overhanging material collapses to form a cliff. Subaerial erosion is considered negligible over the time scales considered.

The sedimentation module computes and redistributes the eroded material, including the bedrock, the notch and the crumbled material overhanging the notch. It operates seawards from the shore, and deposits start at depths greater than critical depth z_0 . Lagoons, if any, are preferentially filled up to depth z_0 with horizontal layers. The remainder is transported further seaward, onto the slope of the fore reef, and is disposed at a rest angle θ (20°).

2.2. Model validation

In order to test the robustness of our model in subsidence mode, we benchmarked modeled reef profiles against the subsiding reef sequences previously modeled in literature (Toomey et al., 2013), namely Hawaii, Oahu and Tahiti, and Molokai. We used the same parameters (foundation slope, maximum growth rate and vertical rate), while using comparable empirical laws, and using our own parameterization elsewhere (eg. Optimum growth depths, z_{\min}). Our model successfully reproduced the modeled morphology of Hawaii, Oahu and Tahiti. It was however impossible to reproduce the barrier of the Molokai reef except when expanding the maximum reef growth depth (z_{\max}) to a higher value than Toomey *et al.* (2013) (down to 25 m). This is probably linked to the differences in the reef accretion model. Following Toomey et al. (2013), we also correctly reproduced the observed reef morphologies using measured parameters from the literature, except for Hawaii where modeled terraces are narrower than observed ones. Graphic results are shown on Fig. DR4. This successful benchmark, together with the ability to reproduce natural cases, validates our modeling approach.

2.3 Parametric analysis

We run ~10,000 simulations to test the impact of several parameters on the reef architecture, including slope (from 0.2 to 2% with 0.1% increments), potential reef growth rate (5 to 15 mm.yr⁻¹ with 1 mm.yr⁻¹ increments), subsidence rate (from 0.6 to 0 mm.yr⁻¹ with 0.05 mm.yr⁻¹ increments). Other parameters remain fixed (Table DR2). Constant subsidence rates, and sea-level variations derived from the sea-level curve (Waelbroeck *et al.*, 2002) were applied within the model. Automated searches of reef morphologies allows for immediate and objective classification. Our algorithm first identifies modern reef crests (set by first occurrence at 2 m bsl.), lagoons (defined as shoreward expanses that are more than 10 m deep and more than 5 m wide) or near-lagunar morphologies (less than 10 m deep and more than 5 m wide), and barriers (reef crest towards the ocean from the lagoon). Fringing reefs are defined as flat expanses, wider than 30 m, where slopes are lower than 0.2 %. The modern reef width is calculated from the modern shoreline to the reef crest. A drowned reef is defined as a wider than 100 m, flat expanse (slopes < 0.2 %). Graphical results are shown in the Fig. DR3.

The islands of the Sunda shelf (Fig. DR2) include the Tin Belt (Riau, Natuna, Karimata, Bangka, Belitung, Tudjuh) in the central and northern regions of the shelf, and Karimunjawa and Baewan at more southeastern locations. All these islands lay over fragments of continental crust, and rise to modest elevations with very low slopes. Only Baewan and Karimunjawa have recent volcanic origins. The reefs the circumscribe the islands of the Java sea (Fig. DR2) are always narrow fringing reefs, which seldom exceed 2 km widths. The local slopes underneath them are always very shallow. These similarities suggest that the coral reef systems may be modeled following similar parametrizations and yield similar results, in particular regarding subsidence rates (within uncertainties, i.e. subsidence rates between 0.2 and 0.3 mm.yr⁻¹).

3. Bathymetry

Bathymetric surveys were conducted using sonar measurements (Humminbird sonar fishfinder 788C) seaward from the modern reef crest at multiple locations in the eastern, northeastern, and northern coasts of Belitung, as well as in the southern coast of Pari island (Seribu archipelago).

4. Sampling in Belitung island and radiocarbon dating

Corals and bivalve shells were ¹⁴C dated at the “Laboratoire de Mesure du Carbone 14” (LMC 14), Saclay, France on the ARTEMIS spectrometer, with procedure and standards described in Dumoulin et al., (2017) and calibrated using IntCal13.14C calibration curve (Reimers *et al.*, 2013). One coral (BEL16-08, *Porites sp.*, 6,490±80 yr BP) and one bivalve (BEL15-3A, *Ostreoidea*, 7,375±60 yr BP) were sampled in the northern part of Belitung Island from an inundated mine pit [2.559198 °S, 107.801502 °E]. One bivalve (BEL15-4, *Tridacna squamosa*, 6,310±90 yr BP) was sampled from a nearby, drained, open tin mine pit [2.552075 °S, 107.804542 °E]. In both sites, samples were extracted at the base of a regressive facies sequence that overlays the intrusive basement (~6 m bsl.), and includes a coral reef (~6 m to 3 m bsl) capped by a beach composed of reef debris, followed by mangrove crab bearing shales (*Macrophthalmus latreillei sp.*, ~3 m to 2 m bsl), a marsh peat (~2 m b.s.l to 1 m b.s.l) and a modern soil. One fossil micro-atoll (BEL16-05, *Porites sp.*, 6,710±50 yr BP) was sampled in life position, on the northern shore of Kalimambang island (2.778740 °S, 107.537148 °E), in the upper intertidal zone (at an elevation of ~0 m).

5. Echosounder surveys

Several surveys have been conducted during the 90s by the Indonesian Marine Geological Institute (now Research and Development Center of Marine Geology / Pusat Penelitian dan Pengembangan Geologi Kelautan, Bandung), and cover most of the Sunda shelf (see location map, Fig. DR1A). The presented profiles (Fig. 2D in the article, and Fig. DR1) have been acquired in 1994 using 500 joules sparker system recorded directly on EPC 3200 Graphic Recorder, which was set to work with 1 second firing rate and 0.5 sec sweep rate.

These unpublished surveys from the central part of the shelf complement the earlier surveys from Darmadi et al., (2007), and Alqahtani et al. (2015) for the northern part of the shelf. All lines display thin layers of sediments associated with Pleistocene transgressions and subsequent regressions that caused local fluvial incisions. Importantly, these layers are undeformed and conform, although separated by episodes of non-deposition. This paraconformity indicates that these layers are uneroded (besides local fluvial incisions). In turn, this shows that all transgressive events are preserved within the sequence.

Up to five layers are found by Darmadi et al., (2007) and Alqahtani et al. (2015) in the northern, deeper part of the shelf, while only two layers can be discerned in the shallowest central part of the shelf, to the North of Belitung island. This comparison points to an earlier onset of inundation of the deeper (~100 m deep) regions with respect to the central part of the shelf (Karimata Strait, Belitung area, ~35 m deep) only because of the original topography, while subsidence occurs at a comparable rate (within uncertainty). Laterally variable rates would not yield comparable stratigraphic layering between the northern shelf and the central part of the shelf.

Figure DR1: A. Location of shallow seismic data surveys in the Java Sea. The red line represents the location of seismic section. The red squares represent location of (1) Alqahtani et al. (2015) and (2) Darmadi et al. (2007) seismic lines. B. Shallow-seismic Parasound profile across the Sunda Shelf, raw and interpreted seismic profile. The basement can be observed onshore on Bangka Island, to the west of the profile, where Triassic sediments (Tanjung Genting Formation) are intruded by Jurassic granite. Top Triassic sediments is limited by a major early Cenozoic erosion surface (e.g., Clements et al., 2011). In this shallow region (~30 m bsl), only two Quaternary transgressions and one level of quaternary incision can be observed. C. Main text, Fig 2D. D. In deeper regions, up to 5 layers are found at greater depths (e.g., Alqahtani et al., 2015, under Creative Commons License)

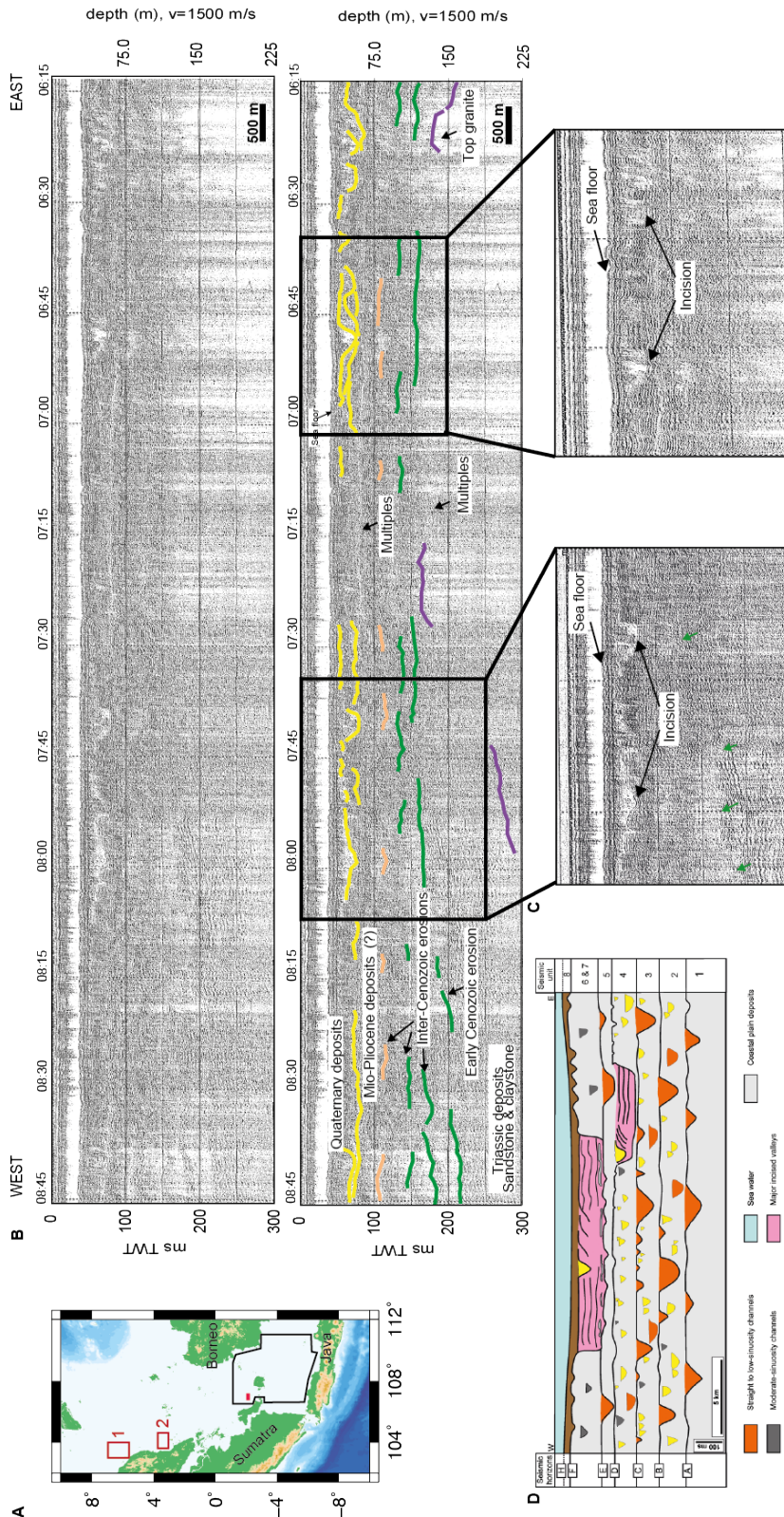
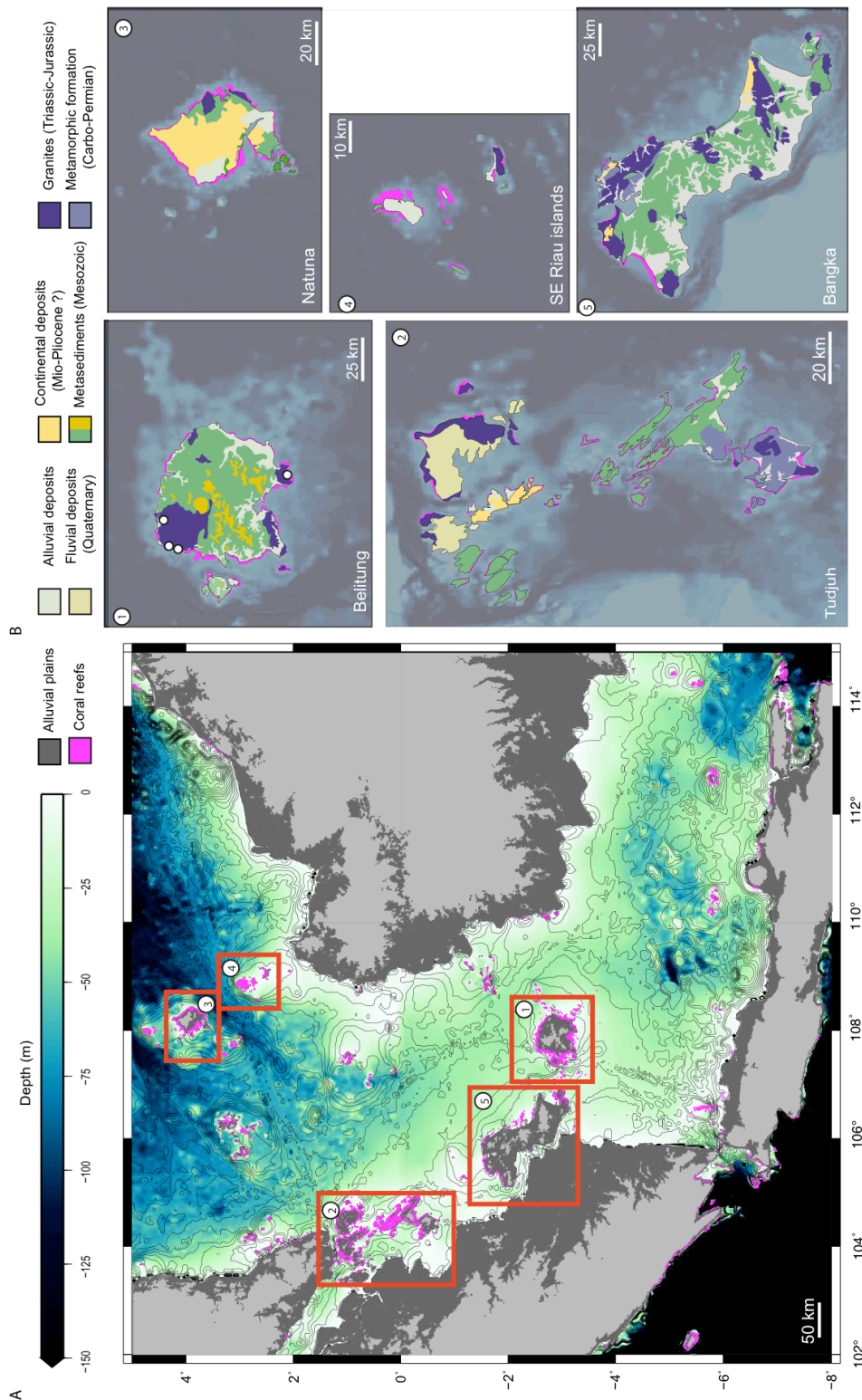


Figure DR2: A. Location of the small islands of the central Sunda shelf. Pink contours underline the location of modern coral reefs extracted from GCRMN database (2011). The map covers $\sim 280,000 \text{ km}^2$, which compares to the size of the shelf itself. B. Simplified geologic maps of Tin Belt islands (from the 1:250 000 geological maps of the Indonesian Geological Survey). All the islands are localised on relatively flat platforms as attested by the bathymetry (color-shaded on the background). Pink contours underline the extent of modern fringing reefs only, as observed on geological maps and satellite images. White circles represent the location of samples dated in this study.



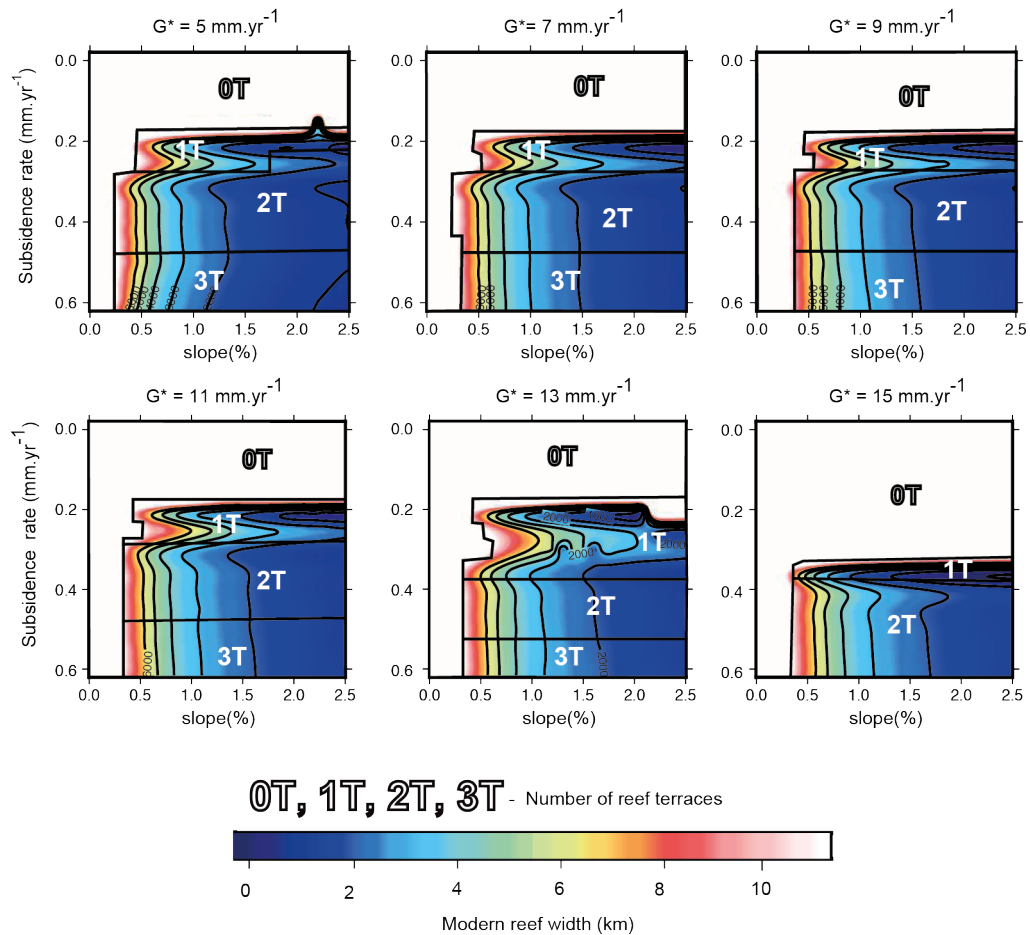


Figure DR3: Additional modelled architectures of reef sequences for various reef growth potential (G^*) slopes, and subsidence rates. Large numbers indicate the number of reef bodies, including the modern reef flat. Color-coded is the width of the modern reef flat. See Table DR2 for parameters

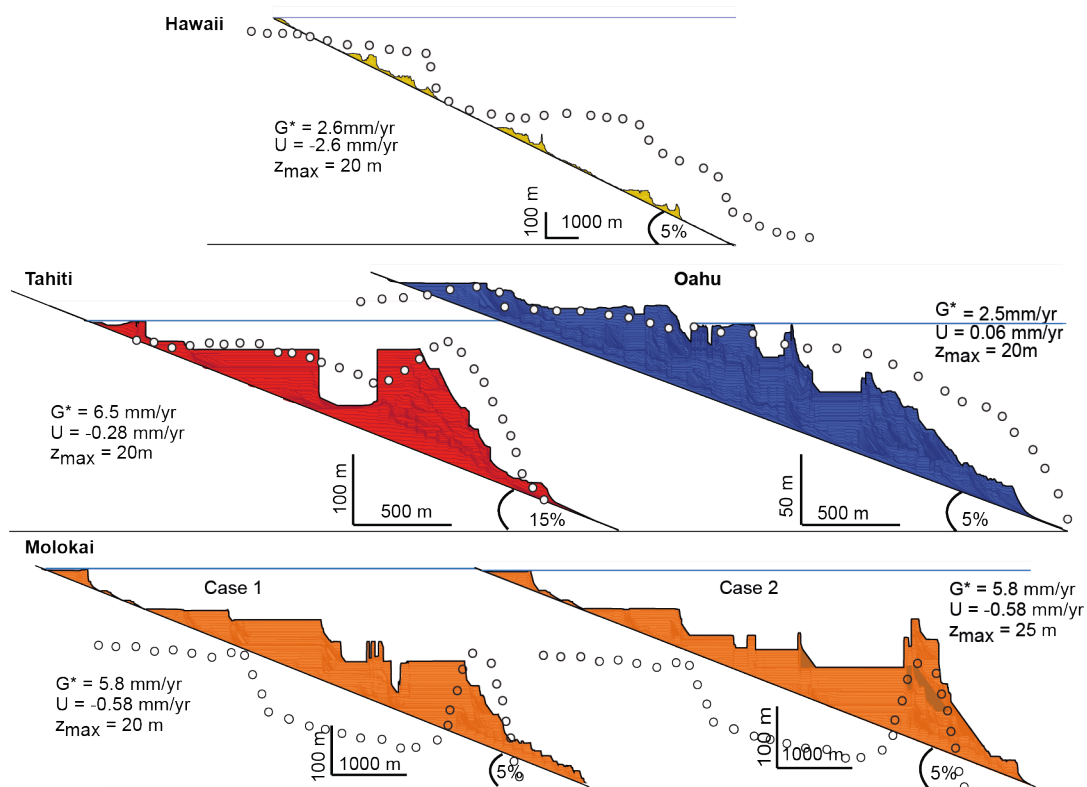


Figure DR4: Model benchmark. Predicted reef morphologies derived from the models using reported reef growth potential (G^*), vertical land motion rate and maximum (U) reef growth depth (z_{max}) (Equation (1)). Model successfully reproduce the predicted reef morphology - drowned terraces for Hawaii, drowned barrier for Tahiti and emerged reef for Oahu - except in the case of Molokai (drowned barrier reef), for which the z_{max} has to be expanded in our model.

Table DR1: Quaternary subsidence and uplift rates in SE Asia (Fig. 1B). Very little information is available for the Sunda shelf: three studies, from Wong *et al.* (2003) and Hanebuth *et al.* (2011) in the northern part of the shelf, and Bird *et al.* (2006), in the Singapore strait, yield comparable rates over similar (Pleistocene) time scales (although the timing of onset remains debatable). Wilson *et al.* (2005) focus in eastern Borneo, at the transition between Sundaland and Wallacea.

Location	Uplift rate (mm yr ⁻¹)	Reference	Methods
Sunda Shelf			
Sunda NE margin	-0.13 to -0.27	Wong <i>et al.</i> (2003)	Seismic stratigraphy
Singapore strait	-0.06 to -0.19	Bird <i>et al.</i> (2006)	Stratigraphy, bathymetry
Northern shelf	-0.25	Hanebuth <i>et al.</i> (2011)	Seismic stratigraphy
Eastern Borneo		Wilson <i>et al.</i> (2005)	
Wallacea			
Alor	0.47	Chappell and Veeh (1978)	U-Series (Uplifted Coral)
Alor	1.10 to 1.20	Hantoro <i>et al.</i> (1994)	U-Series (Uplifted Coral)
Bahari	0.09 ± 0.05	Pedoja <i>et al.</i> (2018)	U-Series (Uplifted Coral)
Buru	0.45	De Smet <i>et al.</i> (1989)	Microfauna/bathymetry
Buton (Sampolawa)	0.14 ± 0.02	Pedoja <i>et al.</i> (2018)	U-Series (Uplifted Coral)
Kisar	0.5	Major <i>et al.</i> (2013)	U-Series (Uplifted Coral)
Rote	1.00 to 1.50	Meritts <i>et al.</i> (1999)	U-Series (Uplifted Coral)
Savu	0.2	Harris <i>et al.</i> (2009)	U-Series (Uplifted Coral)
Semau	0.20 to 0.30	Meritts <i>et al.</i> (1999)	U-Series (Uplifted Coral)
Sulawesi (Luwuk)	0.53-1.84	Sumosusastro <i>et al.</i> (1989)	U-Series (Uplifted Coral)
Sumba (Cape Laundi)	0.49 ± 0.01	Pirazzoli <i>et al.</i> (1993)	U-Series (Uplifted Coral)
Tira	0.12 ± 0.04	Pedoja <i>et al.</i> (2018)	U-Series (Uplifted Coral)
Wangi-Wangi	0.15 ± 0.07	Pedoja <i>et al.</i> (2018)	U-Series (Uplifted Coral)
Buton	0.3 to 1.2	Fortuin <i>et al.</i> (1990)	U-Series (Uplifted Coral)
West Timor (Kupang)	0.30	Jouannic <i>et al.</i> (1988)	U-Series (Uplifted Coral)
Timor	0.8	Tate <i>et al.</i> (2017)	Apatite (U-Th)/He
Sahul shelf			
Scott Reef	-0.29 to -0.45	Collins <i>et al.</i> (2011)	U-Series (Submarine Coral)
Adele Reef	-0.20	Collins and Testa (2010)	U-Series (Submarine Coral)
Cockatoo Island	-0.12	Solihuddin <i>et al.</i> (2015)	U-Series (Submarine Coral)

Table DR2: Coral reef model symbols, parameters and units.

Symbol	Parameter	Values and Units
G^*	Potential reef growth rate	5 to 15 mm.yr ⁻¹
$z_{o\omega}$	Minimal depth for the open water	2 m
z_{max}	Maximum reef growth depth	20 m
z_{min}	Optimal reef growth depth	1 m
γ	Vertical reef growth coefficient	/
ζ	Horizontal reef growth coefficient	/
E^*	Erosional potential	
z_0	Reference depth for wave action	2 m
K	Coefficient of erodibility	0.1 (bedrock)/ 1 (notch)
θ	Critical sediment slope	20°
α	Initial slope	0.2 to 2.5 %
U	Subsidence rate	0.6 to 0 mm.yr ⁻¹

REFERENCES

- Alqahtani, F. A., Johnson, H. D., Jackson, C. A. and Som, M. R. (2015), Nature, origin and evolution of a Late Pleistocene incised valley-fill, Sunda Shelf, Southeast Asia. *Sedimentology*, 62: 1198-1232. <https://doi.org/10.1111/sed.12185>.
- Barber, A. J., Crow, M. J., De Smet, M. E. M., 2005, Sumatra : Geology, resources and tectonic evolution: Geological Society, London, Memoirs, v. 31, p.234-259, <https://doi.org/10.1144/GSL.MEM.2005.031.01.14>
- Bird, M. I., Pang, W. C., Lambeck, K., 2006, The age and origin of the straits of Singapore: *Palaeogeography, Palaeoclimatology, Palaeoecology*, v. 241, p.531–538. <https://doi.org/10.1016/j.palaeo.2006.05.003>
- Chappell, J., Veeh H., 1978, Late quaternary tectonic movements and sea-level changes at Timor and Atauro island: *Geological Society of America Bulletin*, v.89, p.356–368. [https://doi.org/10.1130/0016-7606\(1978\)89<356:LQTMAS>2.0.CO;2](https://doi.org/10.1130/0016-7606(1978)89<356:LQTMAS>2.0.CO;2)
- Clements, B., Burgess, P., M., Hall, R., Cottam, M.A., 2011, Subsidence and uplift by slab-related mantle dynamics: a driving mechanism for the Late Cretaceous and Cenozoic evolution of continental SE Asia: in Hall, R., Cottam, M. A., Wilson, M. E. J. eds., *The SE Asian Gateway: History and Tectonics of the Australia-Asia Collision*: Geological Society, London, Special Publications 355, p. 37-51. <https://doi.org/10.1144/SP355.3>
- Collins, L. B., Testa, V., 2010, Quaternary development of resilient reefs on the subsiding Kimberley continental margin, Northwest Australia: *Brazilian Journal of Oceanography*, v.58, p.67–77. <https://doi.org/10.1590/S1679-87592010000500007>
- Collins, L. B., Testa, V., Zhao, J., Qu, D., 2011, Holocene Growth History and Evolution of the Scott Reef Carbonate Platform and Coral Reef : *Journal of the Royal Society of Western Australia*, v.94, p.239-250
- Darmadi, Y., Willis, B.J., Dorobek, S.L., 2007, Three-Dimensional seismic architecture of fluvial sequences on the low-gradient Sunda shelf, offshore Indonesia: *Journal of Sedimentary Research*, v.77, 225-238. <https://doi.org/10.2110/jsr.2007.024>
- De Smet, M., Fortuin, A., Tjokrosapoetro, S., Van Hinte, J., 1989, Late cenozoic vertical movements of non-volcanic islands in the Banda arc area: *Netherlands Journal of Sea Research*, v.24, p.263–275. [https://doi.org/10.1016/0077-7579\(89\)90153-1](https://doi.org/10.1016/0077-7579(89)90153-1)
- Duffy, B., Kalansky, J., Bassett, K., Harris, R., Quigley, M., van Hinsbergen, D.J.J., Strachan, L. J., Rosenthal, Y., 2017, Mélange versus forearc contributions to sedimentation and uplift, during rapid denudation of a young Banda forearc-continent collisional belt: *Journal of Asian Earth Sciences*, v.138, p.186-210. <https://doi.org/10.1016/j.jseaes.2017.02.008>
- Dumoulin, J.-P. et al., 2017, Status report on sample preparation protocols developed at the LMC14 Laboratory, Saclay, France: from sample collection to ¹⁴C AMS measurement: *Radiocarbon* v.59, p.713-726. <https://doi.org/10.1017/RDC.2016.116>

Fleury, J.-M., Pubellier, M., de Urreiztieta, M. 2007. Structural expression of forearc crust uplift due to subducting asperity. *Lithos*, v.112, p.318-330. <https://doi.org/10.1016/j.lithos.2009.07.007>

Fortuin, A., De Smet, M., Hadiwasastra, S., Van Marle, L., Troelstra, S., and Tjokrosapoetro, S., 1990. Late cenozoic sedimentary and tectonic history of south buton, indonesia. *Journal of Southeast Asian Earth Sciences*, v.4, p.107–124. [https://doi.org/10.1016/0743-9547\(90\)90010-B](https://doi.org/10.1016/0743-9547(90)90010-B)

Giri, C., Ochieng, E., Tiesen, L.L., Zhu, Z., Singh, A., Loveland, T., Masek, J., Duke, N., 2011, Status and distribution of mangrove forests of the world using earth observation satellite data: *Global Ecology and Biogeography*, v.20, p.154-159. <https://doi.org/10.1111/j.1466-8238.2010.00584.x>.

Hanebuth, T. J.J, Voris, H. K., Yokoyama, Y., Saito, Y., Okuno, J., 2011, Formation and fate of sedimentary depocentres on Southeast Asia's Sunda Shelf over the past sea-level cycle and biogeographic implications: *Earth-Science Reviews*, v.104, p.92-110. <https://doi.org/10.1016/j.earscirev.2010.09.006>

Hantoro, W., Pirazzoli, P. A., Jouannic, C., Faure, H., Hoang, C. T., Radtke, U., Causse, C., Borel Best, M., Lafont, R., Bieda, S., Lambeck, K., 1994, Quaternary uplifted coral reef terraces on Alor island, East Indonesia: *Coral reefs*, v.13, p.215–223.

Harris, R., Vorkink, M. W., Prasetyadi, C., Zobell, E., Roosmawati, N., Apthorpe, M., 2009, Transition from subduction to arc-continent collision : Geologic and neotectonic evolution of Savu Island, Indonesia : *Geosphere*, v.5, p. 152-171. <https://doi.org/10.1130/GES00209.1>

Husson, L., Pastier, A-M., Pedroja, K., Elliot, M., Paillard, D., Authemayou, C., Sarr, A-C., Schmitt, A., Cahyarini, S.Y., 2018. Reef carbonate productivity during Quaternary sea level oscillations: *Geochemistry, Geophysics, Geosystems*, published online. <https://doi.org/10.1002/2017GC007335>

Jouannic, C., Hoang, C. T., Hantoro, W. S., Delinom, R. M., 1988, Uplift rate of coral reef terraces in the area of Kupang, West Timor: preliminary results: *Palaeogeography, Palaeoclimatology, Palaeoecology*, v.68, p.259–272. [https://doi.org/10.1016/0031-0182\(88\)90044-2](https://doi.org/10.1016/0031-0182(88)90044-2)

Major, J., Harris, R., Chiang, H.-W., Cox, N., Shen, C. C. Nelson, S. T., Prasetyadi, C., Rianto, A., 2013, Quaternary hinterland evolution of the active Banda arc: Surface uplift and neotectonic deformation recorded by coral terraces at Kisar, Indonesia: *Journal of Asian Earth Sciences*, v.73, p.149–161. <https://doi.org/10.1016/j.jseaes.2013.04.023>

Mansor, M.Y., Rahman, A.H.A., Menier, D., Pubellier, M., 2014, Structural evolution of Malay Basin, its link to Sunda Block tectonics, *Marine and Petroleum Geology*, v.58, p. 736-748. <https://doi.org/10.1016/j.marpetgeo.2014.05.003>

Merritts, D., Eby R., Harris, R., Edwards, R. L., Chang, H., 1999, Variable rates of late quaternary surface uplift along the Banda arc-australian plate collision zone, Eastern Indonesia: *Geological Society, London, Special Publications*, v.146, p.213–224. <https://doi.org/10.1144/GSL.SP.1999.146.01.12>

Nguyen, N., Duffy, B., Shulmeister, J., Quigley, M., 2013, Rapid Pliocene uplift in Timor : *Geology*, v. 41, p. 179-182, <https://doi.org/10.1130/G33420.1>

Pedoja, K., Husson, L., Bezos, A., Pastier, A-M., Imran, A-M., Arias, C., Sarr, A-C., Elliot, M., Pons-Branchu, E., Regard, E., Nexer, M., Regard, V., Hafidz, A., Robert, X., Benoit, L., Delcaillau, B., Authemayou, C., Dumoulin, C., Choblet, G., 2018, On the long-lasting sequences of coral reef terraces from SE Sulawesi (Indonesia): distribution, formation, and global significance. *Quaternary Science Reviews*, v.188, p37-57. <https://doi.org/10.1016/j.quascirev.2018.03.033>

Pirazzoli, P. A., Radtke, U., Hantoro, W. S., Jouannic, C., Hoang, C. T., Causse, C., Borel Best, C., 1993, A one million-year-long sequence of marine terraces on sumba island, Indonesia: *Marine Geology*, v.109, p.221–236. [https://doi.org/10.1016/0025-3227\(93\)90062-Z](https://doi.org/10.1016/0025-3227(93)90062-Z)

Pholbud, P., Hall, R., Advokaat, E., Burgess, P., Rudyawan, A., 2012. A new interpretation of Gorontalo Bay, Sulawesi : *Indones. Pet. Assoc. Proc. 36th Annu. Conv.*, IPA12-G-039 p. 1-23.

Pubellier, M and Morley, C..K., 2014, The basins of Sundaland (SE Asia): Evolution and boundary conditions: *Marine and Petroleum Geology*, v. 58, p. 555-578. <https://doi.org/10.1016/j.marpetgeo.2013.11.019>

Reimer, P. J. et al., 2013, IntCal13 and MARINE13 radiocarbon age calibration curves 0-50,000 years calBP: *Radiocarbon*, v.55, p.1869-1887. https://doi.org/10.2458/azu_js_rc.55.16947

Roosmawati, N., Harris, R., 2009, Surface uplift history of the incipient Banda arc-continent collision : *Geology and synorogenic foraminifera of Rote and Savu Islands, Indonesia : Tectonophysics*, v. 479, p. 95-110, <https://doi.org/10.1016/j.tecto.2009.04.009>

Sandiford, M., 2008, Seismic moment release during slab rupture beneath the Banda Sea, *Geophysical Journal International*, v. 174, p. 659-671. <https://doi.org/10.1111/j.1365-246X.2008.03838.x>

Solihuddin, T., Collins, L. B., Blakeway, D., O’Leary, M. J., 2015, Holocene coral reef growth and sea level in a macrotidal, high turbidity setting: Cockatoo Island, Kimberley Bioregion, northwest Australia: *Marine Geology*, v.359, p.50-60. <https://doi.org/10.1016/j.margeo.2014.11.011>

Spencer, C. J., Harris, R., Major, J.T., 2016, Provenance of Permian-Triassic Gondwana Sequence units accreted to the Banda Arc in the Timor region: Constraints from zircon U-Pb and Hf isotopes: *Gondwana Research*, v.38, p.28-39. <https://doi.org/10.1016/j.gr.2015.10.012>

Sumosusastro P., Tjia H., Fortuin A., Van Der Plicht J., 1989, Quaternary reef record of differential uplift at Luwuk, Sulawesi East arm, Indonesia: *Netherlands Journal of Sea Research*, v.24, p.277–285. [https://doi.org/10.1016/0077-7579\(89\)90154-3](https://doi.org/10.1016/0077-7579(89)90154-3)

Tate, G. W., McQuarrie, N., Tiranda, H., van Hinsbergen, D. J. J., Harris, R., Zachariasse, W.J., Fellin, M.G., Reiners, P.W. and Willett, S.D., 2017, Reconciling regional continuity with local variability in structure, uplift and exhumation of the Timor orogen : *Gondwana Research*, v.49, p. 364-386. <https://doi.org/10.1016/j.gr.2017.06.008>

Toomey, M., Ashton, A. D., Perron, T., 2013. Profiles of ocean island coral reefs controlled by sea-level history and carbonate accumulation rates: *Geology*, v.41, p.731-734.
<https://doi.org/10.1130/G34109.1>

Waelbroeck, C., Labeyrie, L., Michel, E., Duplessy, J. C., McManus, J. F., Lambeck, K., Balbon, E., Labracherie, M., 2002, Sea-level and deep water temperature changes derived from benthic foraminifera isotopic records: *Quaternary Science Reviews*, v. 21, p.295–305.
[https://doi.org/10.1016/S0277-3791\(01\)00101-9](https://doi.org/10.1016/S0277-3791(01)00101-9)

Wilson, M. E. (2005). Development of equatorial delta-front patch reefs during the Neogene, Borneo. *Journal of Sedimentary Research*, v.75(1), p.114-133.

Wong, H. K., Lüdmann, T., Haft, C., Paulsen, A-M., 2003, Quaternary sedimentation in the Molengraaff paleo-delta, northern Sunda-shelf (Southern South China Sea): *SEPM Special Publication*, v.76, p.201-216.